Optical Aspects of the Interaction of Focused Beams with Plasmonic Nanoparticles

Kürşat Şendur

Faculty of Engineering and Natural Sciences
Sabancı University, Istanbul, 34956, Turkey
sendur@sabanciuniv.edu

Abstract **─** In this study, the interaction of nano-particles with focused beams of various angular spectra is investigated. This study demonstrates that the focused light can be used to manipulate the near-field radiation around nanoparticles. It is shown that suppressing strong lobes and enhancing weaker lobes is possible for spherical particles by altering the angular spectrum. This can have an impact on plasmonic applications where strong and weak fields are desired at specific locations.

Index Terms **─** Nanoparticles, nanoscale, plasmonics, radiative energy transfer, scattering, surface plasmons.

I. INTRODUCTION

Surface plasmons [1-2], optical nanoantennas [3-6], and radiative energy transfer at the nanoscale [7-9] have led to significant advances in nanotechnology. Plasmonics and interaction of light with nanoparticles have fascinated scientists because of their ability to manipulate light beyond the diffraction limit. Such an achievement at the nanoscale has enabled scientists to overcome technological barriers and expand the frontiers for scientific breakthroughs in near-field imaging [10], solar cells [11], optical data storage [12], heat assisted magnetic recording [13], light emitting devices [14], spectroscopy [15], medical applications [16], and bio-chemical sensors [17].

The interest in the interaction of photons with metallic nanoparticles for emerging nanotechnology applications is driven mainly due to the large enhancement and tight localization of electromagnetic fields in the vicinity of nanoparticles. Although there has been much effort to understand the effects of various parameters on the plasmon resonances of nanoparticles, the interaction of nanoparticles with a focused beam of light has not been significantly investigated in the context of particle plasmons. Similarly, the interaction of a tightly focused beam of incident light with metallic prolate spheroids has also been largely overlooked in the literature.

In this study, we investigate the effect of the angular spectrum of a focused beam of light on the near-field radiation from spherical nanoparticles and prolate spheroids. This paper is an extended version of previous conference papers [18, 19]. Focused beams with various angular spectra are used in this study to understand field distributions and their formations over the nanoparticles.

II. RICHARDS-WOLF VECTOR FIELD FORMALISM

To obtain an accurate representation of a tightly focused beam of light, the theory established by Richards and Wolf [20, 21] is used. In this approach, rays that are incident onto a lens are collected and focused based on the rules of geometric optics. After each ray is diffracted by the lens system, the overall contribution is calculated by summing up the individual rays. Formulas based on the Richards and Wolf vector field theory have been previously used in the literature [22-25] for focused beams of various polarizations.

A linearly polarized beam in the x-direction, which is focused onto the x-y plane and propagating in the z-direction is used. The beam is cylindrically symmetric around the z-axis with the focal point at (0, 0, 0). The incident electric field near the focus is given as [24]

Submitted On: Oct. 15, 2011
Accepted On: Jan. 25, 2012

$$\vec{E}(\vec{r}) = -\frac{i}{\lambda}\int_0^{\alpha}\int_0^{2\pi} \vec{a}(\theta,\phi)e^{i\vec{k}\cdot\vec{r}}\sin\theta\, d\phi\, d\theta\,, \quad (1)$$

for a linearly polarized focused beam, where α is the half angle of the beam, r is the observation point, and

$$\vec{a}(\theta,\phi) = \begin{bmatrix} \cos\theta\cos^2\phi + \sin^2\phi \\ \cos\theta\cos\phi\sin\phi - \cos\phi\sin\phi \\ \sin\theta\cos\phi \end{bmatrix}\sqrt{\cos\theta}\,. \quad (2)$$

The half-beam angle α, which defines the upper limit of the integral in Eq. (1), represents the span of angles at which the corresponding plane wave has a non-zero contribution to the focused field. The half-beam angle is illustrated in Fig. 1. Any lens has a finite size, which results in the integral in Eq. (1) having an upper limit α. The half-beam angle is determined by the physical configuration and the size of the lens system. The largest α used in this study is 60°, which yields a full-width half-maximum beam waist of 405 nm at a 700 nm wavelength. The amplitude of the focused beam is normalized so that the value at the focus is 1 V/m.

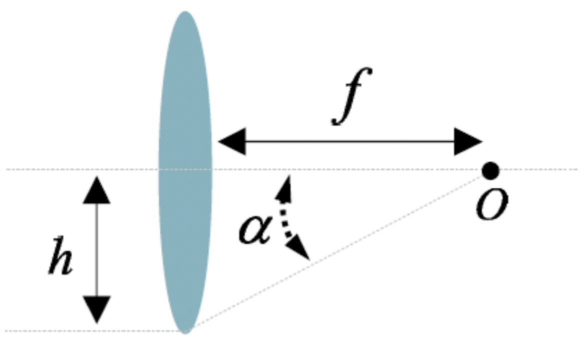

Fig. 1. A graphical illustration of the half-beam angle, α. The focus of the lens is illustrated with the point *O*.

The spatial distributions of incident focused beams are plotted in Fig. 2 for various α. The results in Fig. 2 illustrate the field distributions in the absence of a metallic particle. The results in subsequent figures illustrate the impact of placing a spherical nanoparticle on the electric field distributions. In Figs. 2(a), (c), and (e), the *x*-component of the electric field $E_x(x, y, 0)$ is plotted on the *x-y* plane for α=0°, α=30°, and α=60°, respectively. The beam with α=0° corresponds to a plane wave. As α is increased, the beam becomes more tightly focused. Similarly in Figs. 2(b), (d), and (f), the *x*-component of the electric field $E_x(x, 0, z)$ is plotted on the *x-z* plane for α=0°, α=30°, and α=60°, respectively. The field distribution is elongated in the *z*-direction due to the poor axial resolution of lenses [22].

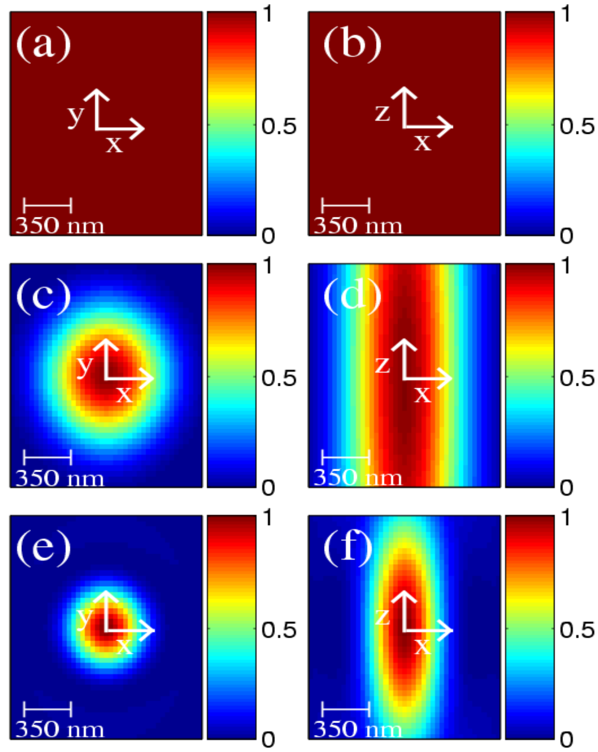

Fig. 2. (a) $E_x(x, 0, z)$ on the *x-y* plane for α = 0°, (b) $E_x(x, 0, z)$ on the *x-z* plane for α = 0°, (c) $E_x(x, 0, z)$ on the *x-y* plane for α = 30°, (d) $E_x(x, 0, z)$ on the *x-z* plane for α =30°, (e) $E_x(x, 0, z)$ on the *x-y* plane for α = 60°, and (f) $E_x(x, 0, z)$ on the *x-z* plane for α =60°.

In the representation in Eq. (1), each ray is identified by angles θ and φ depending on their incidence angle. Only the rays incident on the lens can be collected. The rays beyond the size of the lens cannot be focused by the lens system. The half-beam angle imposes a cut-off for the upper limit of the integral in Eq. (1). Therefore, the half-beam angle incorporates the physics of the lens system into Eq. (1). The finite size of the lens results in the integral in Eq. (1) having an upper limit θ = α where α ≤ 90°. If the size of the lens approaches to infinity, the upper limit of the integral in Eq. (1) will approach to 90°. To study the interaction of nanoparticles with incident beams with different angular spectra, the half beam angle will be varied.

III. RESULTS

The plasmon resonances of nanoparticles have been investigated in the literature to understand the effects of various parameters [26] and to engineer the spectral response [27-29]. Until recently, the interaction of nanoparticles with a focused beam of light has not been significantly investigated in the context of particle plasmons. With emerging potential applications, there is an increased interest in the interaction of focused beams and nanoparticles [25, 30-38] as well as developing computational solutions to numerical aspects of scattering problems [39, 40]. To analyze the effect of the angular spectrum, a silver nanoparticle is illuminated using a focused beam of light with small and large α. The focused beam propagates in the z-direction, and is polarized in the x-direction.

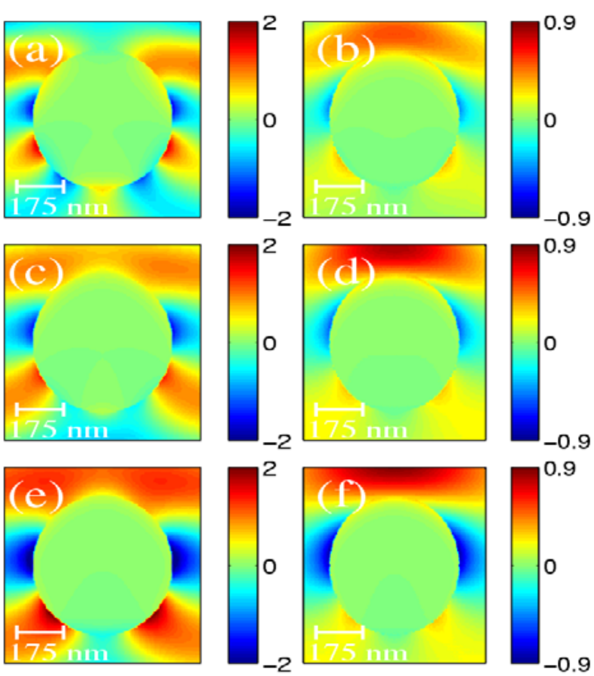

Fig. 3. $E_x(x, 0, z)$ on the x-z plane for various [α (°), λ (nm)]: (a) $E_x(x, 0, z)$ for [5, 400], (b) $E_x(x, 0, z)$ for [60, 400], (c) $E_x(x, 0, z)$ for [5, 500], (d) $E_x(x, 0, z)$ for [60, 500], (e) $E_x(x, 0, z)$ for [5, 600], and (f) $E_x(x, 0, z)$ for [60, 600].

In Fig. 3, the electric field is computed at various wavelengths on the x-z plane for a silver sphere with a 250 nm radius. The field distribution $E_x(x, 0, z)$ is plotted for α=5° and α=60°. A comparison of Figs. 3(a) and (b) suggests that the field distribution at λ = 400 nm for α=5° shows a significant difference compared to the results of α=60°. In Figs. 3(c)-(f), deviations are observed at other wavelengths as well. The $E_y(x, 0, z)$ component is negligible for the solutions. The impact of altering the angular spectrum is more drastic for the $E_z(x, 0, z)$ component, as shown in Fig. 4. For example, when the angular spectrum is narrowly distributed along the direction of propagation, as shown in Fig. 4(e), two stronger lobes are observed at the back of the spherical particle. As α is increased, and therefore the angular spectrum is widened, the stronger lobes are moved from the back of the particle to the front of the particle, as shown in Fig. 4(f). This was achieved without changing the frequency, geometry, or composition of the particle.

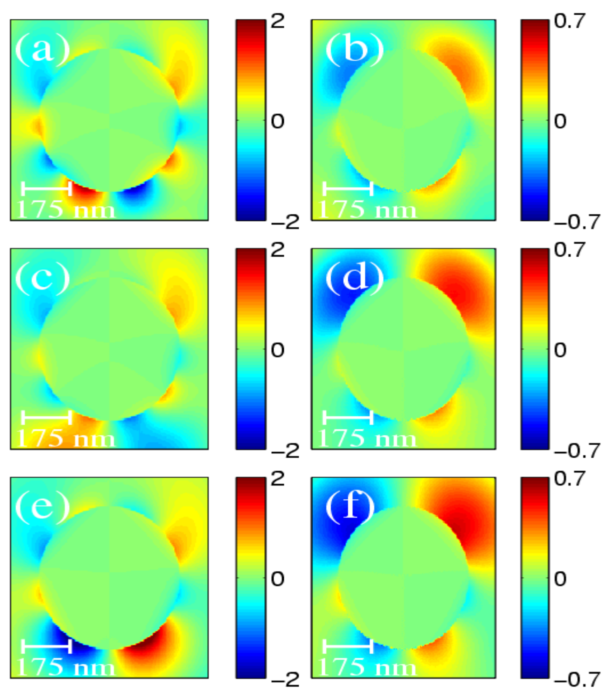

Fig. 4. $E_z(x, 0, z)$ on the x-z plane for various [α(°), λ (nm)]: (a) $E_z(x, 0, z)$ for [5, 400], (b) $E_z(x, 0, z)$ for [60, 400], (c) $E_z(x, 0, z)$ for [5, 500], (d) $E_z(x, 0, z)$ for [60, 500], (e) $E_z(x, 0, z)$ for [5, 600], and (f) $E_z(x, 0, z)$ for [60, 600].

The results in Figs. 3 and 4 demonstrate that suppressing strong lobes and enhancing weaker lobes is possible by altering the angular spectrum. These results have important implications for plasmonic applications. Some plasmonic applications require strong fields at specific locations. For example, in heat assisted magnetic recording (HAMR) [13] strong fields are necessary at the air-bearing surface [41] to change the magnetic properties of the recording medium. The results in this study suggest that the location of strong fields, such as the air-bearing fields used in HAMR, can be adjusted using the angular spectrum of the incident field. Additional potential applications include single molecule spectroscopy [42, 43], single molecule fluorescence enhancement [44], plasmonic waveguides [45-47], directional plasmonic emitters [48-50], plasmonic routers and switches, which can benefit from manipulating the location of strong optical spots using the angular spectrum of the incident beam.

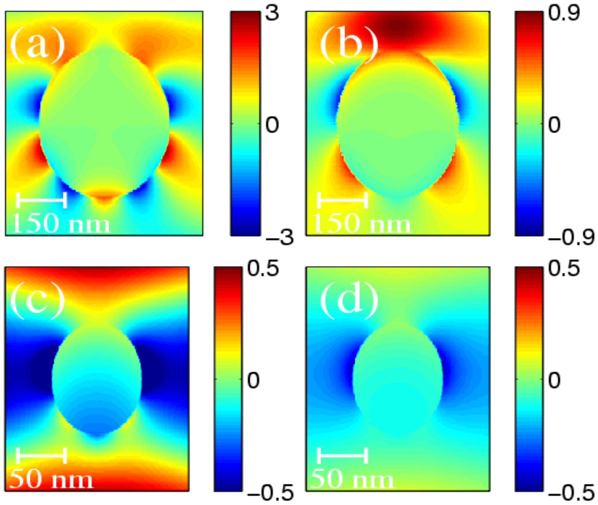

Fig. 5. $E_x(x, 0, z)$ on the *x-z* plane for various [α (°), r (nm)]: (a) [5, 200], (b) [60, 200], (c) [5, 50], and (d) [60, 50].

$E_x(x, 0, z)$ and $E_z(x, 0, z)$ are plotted for various particle sizes at λ = 400 nm in Figs. 5 and 6, respectively. The results suggest that the $E_x(x, 0, z)$ and $E_z(x, 0, z)$ distributions vary for small and large α, even when the particle size is small. The difference becomes smaller as the particle size decreases. If a particle smaller than λ/10 is placed at the focus of a tightly focused beam of light, the interaction becomes quasistatic. Therefore, for small particles the results of the small and large α begin to resemble each other. For very small particles smaller than λ/10, the nanoparticle is not impacted by the wide range of spectral components, even if the incident light has a wide angular spectrum. A very small particle does not feel the variation in the field, since it is much smaller than the variations shown in Fig. 2. However, as the sphere gets larger it will start to interact with various components of the angular spectrum.

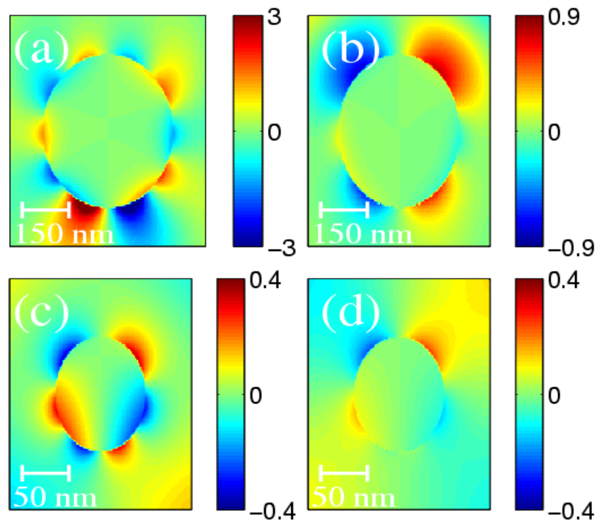

Fig. 6. $E_z(x, 0, z)$ on the *x-z* plane for various [α (°), r (nm)]: (a) [5, 200], (b) [60, 200], (c) [5, 50], and (d) [60, 50].

Figure 7(a) shows the results for a linearly polarized plane wave at the incidence angle 0°. Figures 7(b)-(d) illustrate the results for a linearly polarized focused wave with half beam angles of 5°, 45°, and 60°. A comparison of Figs. 7(a) and (b) suggests that the result of the small α is similar to that of a plane wave at θ = 0°. Figures 7(c) and (d) show that the plasmon distribution for a large α deviates from that of a plane wave. This deviation can be interpreted using Figs. 7(a), (e), and (f). As shown in Figs. 7(a), (e), and (f), the field distribution changes for plane waves of different incidence angles. Plane waves with different angles are scaled and summed up based on the angular spectrum of the focused beam. For small half-beam angle α, the plane wave at an incidence angle 0° is the dominant contributor, as shown in Fig. 7(b). Contributions from larger incidence angles start to dominate as the angular spectrum gets wider, which impacts the distributions in Figs. 7(c) and (d).

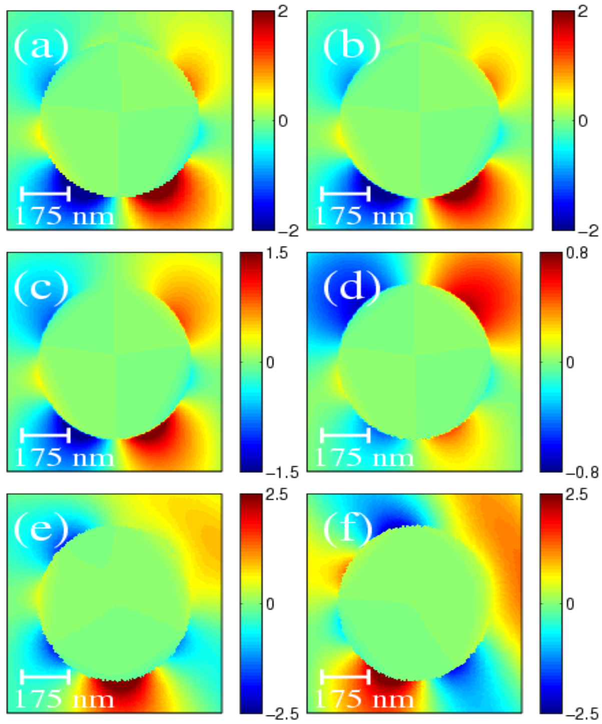

Fig. 7. $E_z(x, 0, z)$ on the x-z plane: (a) plane wave at 0°, (b) focused beam with α = 0°, (c) focused beam with α = 45°, (d) focused beam with α = 60°, (e) plane wave at 30°, and (f) plane wave at 60°.

Although the field distributions over the spheres resulting from off-angle plane waves in Figs. 7(e) and (f) are asymmetric, the field distributions over spheres excited with focused beams in Fig. 7 are symmetric. The primary reason why the asymmetry in the results in Figs. 7(e) and (f) does not result in asymmetry in the focused beam results can be explained as follows: In Figs. 7(e) and (f), the results for the plane waves with non-zero incidence angles are presented in the global coordinate system, in which the results are asymmetric. For a plane wave with a non-zero incidence angle, however, the results are symmetric in the rotated coordinate system, which is rotated by the incidence angle with respect to the global coordinate system. The asymmetry in the individual plane wave results is not reflected in the focused beam results, because for each (θ, ϕ) ray, there is a corresponding (θ, ϕ+π) ray. The sum of these rays, each of which are asymmetric in the global x-z coordinate system, result in a symmetric distribution. Therefore, the asymmetry of the individual components shown in Figs. 7(e) and (f) do not result in asymmetry in the focused beam results.

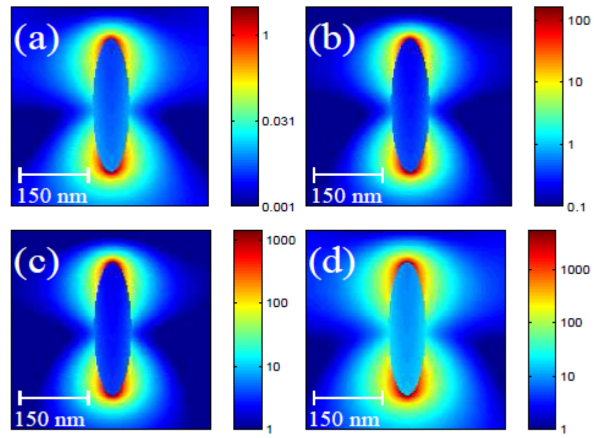

Fig. 8. Intensity distributions for a prolate spheroid. The distributions are given for various half-beam angles: (a) α = 15°, (b) α = 30°, (c) α = 45°, and (d) α = 60°.

In Fig. 8, the impact of the angular spectrum distribution of the incident beam on the near-field radiation of a prolate spheroidal nanoparticle is studied. In Fig. 8, the total intensity profile is plotted on the x-z plane, which passes through the center of a prolate spheroid particle with a major/minor axis ratio of 5. Intensity distributions for a prolate spheroid are given for various half-beam angles. In this figure, the prolate spheroids are illuminated with a radially focused beam with half-beam angles α = 15°, α = 30°, α = 45°, and α = 60° The field distributions in Fig. 8 are normalized to the value of the incident intensity at the focus. The results suggest that the electric field distribution does not change as the half-beam angle is increased. The amplitude of the near field electric field distribution, however, increases as the half-beam angle is increased. The angular spectrum of the incident beam is tight for α = 15°, becoming wider as the half beam angle is increased. Therefore, the incident wave amplitude onto the particle and resulting total field amplitude increases as the half-beam angle increases.

VI. CONCLUSION

In summary, the angular spectrum of the incident beam had a significant impact on the plasmon distribution of nanoparticles. Beams with narrow and wide angular spectra interacted differently with a nanoparticle. For a focused beam with a small α, the results were similar to those of a plane wave. As α was increased, the results differed significantly from those of a plane wave. The results suggest that it is possible to manipulate plasmon distributions by adjusting the angular spectrum of an incident focused beam. On the other hand, for prolate spheroids the electric field distribution does not change as the half-beam angle is increased. The amplitude of the near-field electric field distribution, however, increases as the half-beam angle is increased.

ACKNOWLEDGMENT

This work is supported by TÜBİTAK project numbers 108T482 and 109T670 and by a European Community Marie Curie International Reintegration Grant (IRG) to Kürşat Şendur (MIRG-CT-2007-203690). Kürşat Şendur acknowledges partial support from the Turkish Academy of Sciences. The author acknowledges the assistance of undergraduate students Eren Ünlü, Ahmet Şahinöz, Mert Gülhan, and Serkan Yazıcı in preparing CAD files for the simulations.

REFERENCES

[1] W. L. Barnes, A. Dereux, and T. W. Ebbesen, “Surface Plasmon Subwavelength Optics,” *Nature*, vol. 424, pp. 824-830, 2003.

[2] T. W. Ebbesen, H. J. Lezec, H. F. Ghaemi, T. Thio, and P. A. Wolff, “Extraordinary Optical Transmission through Sub-Wavelength Hole Arrays,” *Nature*, vol. 391, pp. 667-669, 1998.

[3] P. Bharadwaj, B. Deutsch, and L. Novotny, “Optical Antennas,” *Adv. Opt. Photon.*, vol. 1, pp. 438-483, 2009.

[4] L. Novotny and N. van Hulst, “Antennas for Light,” *Nature Photon.*, vol. 5, pp. 83-90, 2011.

[5] H. Fischer and O. J. F. Martin, “Engineering the Optical Response of Plasmonic Nanoantennas,” *Opt. Express*, vol. 16, pp. 9144-9154 (2008).

[6] L. Novotny, “Effective Wavelength Scaling for Optical Antennas,” *Phys. Rev. Lett.*, vol. 98, pp. 266802, 2007.

[7] E. Rousseau, A. Siria, G. Jourdan, S. Volz, F. Comin, J. Chevrier, and J.-J. Greffet, “Radiative Heat Transfer at the Nanoscale,” *Nature Photon.*, vol. 3, pp. 514-517, 2009.

[8] S. Shen, A. Narayanaswamy, and G. Chen, “Surface Phonon Polariton Mediated Energy Transfer between Nanoscale Gaps,” *Nano Lett.*, vol. 9, pp. 2909-2913, 2009.

[9] M. Francoeur, M. P. Menguc, and R. Vaillon, “Near-Field Radiative Heat Transfer Enhancement via Surface Phonon Polaritons Coupling in Thin Films,” *Appl. Phys. Lett.*, vol. 93, pp. 043109, 2008.

[10] A. Hartschuh, E. J. Sanchez, X. S. Xie, and L. Novotny, “High-Resolution Near-Field Raman Microscopy of Single-Walled Carbon Nanotubes,” *Phys. Rev. Lett.*, vol. 90, pp. 095503, 2003.

[11] H. Atwater and A. Polman, “Plasmonics for Improved Photovoltaic Devices,” *Nat. Mater.*, vol. 9, pp. 205-213, 2010.

[12] C. Peng, “Surface-Plasmon Resonance of a Planar Lollipop Near-Field Transducer,” *Appl. Phys. Lett.*, vol. 94, pp. 171106, 2009.

[13] K. Sendur, C. Peng, and W. Challener, “Near-Field Radiation from a Ridge Waveguide Transducer in the Vicinity of a Solid Immersion Lens,” *Phys. Rev. Lett.*, vol. 94, pp. 043901, 2005.

[14] X. Gu, T. Qiu, W. Zhang, and P. K. Chu, “Light-Emitting Diodes Enhanced by Localized Surface Plasmon Resonance,” *Nanoscale Res. Lett.*, vol. 6, pp. 199, 2011.

[15] K. A. Willets and R. P. V. Duyne, “Localized Surface Plasmon Resonance Spectroscopy and Sensing,” *Annu. Rev. Phys. Chem.*, vol. 58, pp. 267-297, 2007.

[16] A. M. Gobin, M. H. Lee, N. J. Halas, W. D. James, R. A. Drezek, and J. L. West, “Near-Infrared Resonant Nanoshells for Combined Optical Imaging and Photothermal Cancer Therapy,” *Nano Lett.*, vol. 7, pp. 1929-1934, 2007.

[17] N. Liu, M. L. Tang, M. Hentschel, H. Giessen, and A. P. Alivisatos, “Nanoantenna-Enhanced Gas Sensing in a Single Tailored Nanofocus,” *Nat. Mater.*, vol. 10, pp. 631-636, 2011.

[18] K. Sendur, A. Şahinoz, E. Unlu, S. Yazici, and M. Gulhan, “Near-Field Radiation from Nano-Particles and Nano-Antennas Illuminated with a Focused Beam of Light,” in *Materials for Nanophotonics — Plasmonics, Metamaterials and Light Localization*, edited by M. Brongersma, L. Dal Negro, J. M. Fukumoto, L. Novotny (Mater. Res. Soc. Symp. Proc. Volume 1182, Warrendale, PA, 2009), 1182-EE16-03.

[19] K. Sendur, “Optical Aspects of the Interaction of Focused Beams with Plasmonic Nanoparticles,” *Proceedings of the International Workshop on Computational Electromagnetics*, Izmir, Turkey, August 2011.

[20] E. Wolf, “Electromagnetic Diffraction in Optical Systems I. An Integral Representation of the Image Field,” *Proc. Roy. Soc. London Ser. A*, vol. 253, pp. 349-357, 1959.

[21] B. Richards and E. Wolf, “Electromagnetic Diffraction in Optical Systems II. Structure of the

Image Field in an Aplanatic System," *Proc. Roy. Soc. London Ser. A*, vol. 253, pp. 358-379, 1959.

[22] L. Novotny and B. Hecht, *Principles of Nano-Optics*, Cambridge University Press, New York, 2006.

[23] K. S. Youngworth and T. G. Brown, "Focusing of High Numerical Aperture Cylindrical-Vector Beams," *Opt. Express*, vol. 7, pp. 77-87, 2000.

[24] I. Ichimura, S. Hayashi, and G. S. Kino, "High-Density Optical Recording using a Solid Immersion Lens," *Appl. Opt.*, vol. 36, pp. 4339-4348, 1997.

[25] W. A. Challener, I. K. Sendur, and C. Peng, "Scattered Field Formulation of Finite Difference Time Domain for a Focused Light Beam in a Dense Media with Lossy Materials," *Opt. Express*, vol. 11, pp. 3160-3170 (2003).

[26] K. L. Kelly, E. Coronado, L. L. Zhao, and G. C. Schatz, "The Optical Properties of Metal Nanoparticles: The Influence of Size, Shape, and Dielectric Environment," *J. Phys. Chem. B*, vol. 107, pp. 668–677, 2003.

[27] S. J. Oldenburg, R. D. Averitt, S. L. Westcott, and N. J. Halas, "Nanoengineering of Optical Resonances," *Chem. Phys. Lett.*, vol. 288, pp. 243-247, 1998.

[28] E. Prodan, C. Radloff, N. J. Halas, and P. Nordlander, "A Hybridization Model for the Plasmon Response of Complex Nanostructures," *Science*, vol. 302, pp. 419-422, 2003.

[29] P. Nordlander, C. Oubre, E. Prodan, K. Li, and M. I. Stockman, "Plasmon Hybridization in Nanoparticle Dimers," *Nano Lett.*, vol. 4, pp. 899-903, 2004.

[30] K. Sendur, W. Challener, and O. Mryasov, "Interaction of Spherical Nanoparticles with a Highly Focused Beam of Light," *Opt. Express*, vol. 16, pp. 2874-2886, 2008.

[31] J. Lerme, G. Bachelier, P. Billaud, C. Bonnet, M. Broyer, E. Cottancin, S. Marhaba, and M. Pellarin, "Optical Response of a Single Spherical Particle in a Tightly Focused Light Beam: Application to the Spatial Modulation Spectroscopy Technique," *J. Opt. Soc. Am. A*, vol. 25, pp. 493-514, 2008.

[32] N. M. Mojarad, V. Sandoghdar, and M. Agio, "Plasmon Spectra of Nanospheres under a Tightly Focused Beam," *J. Opt. Soc. Am. B*, vol. 25, pp. 651-658, 2008.

[33] D. Khoptyar, R. Gutbrod, A. Chizhik, J. Enderlein, F. Schleifenbaum, M. Steiner, and A. J. Meixner, "Tight Focusing of Laser Beams in a λ/2-Microcavity," *Opt. Express*, vol. 16, pp. 9907-9917, 2008.

[34] A. V. Failla, H. Qian, H. H. Qian, A. Hartschuh, and A. J. Meixner, "Orientational Imaging of Subwavelength Au Particles with Higher Order Laser Modes," *Nano Lett.*, vol. 6, pp. 1374-1378, 2006.

[35] N. M. Mojarad and M. Agio, "Tailoring the Excitation of Localized Surface Plasmon-Polariton Resonances by Focusing Radially-Polarized Beams," *Opt. Express*, vol. 17, pp. 117-122, 2009.

[36] K. Sendur, "An Integral Equation Based Numerical Solution for Nanoparticles Illuminated with Collimated and Focused Light," *Opt. Express*, vol. 17, pp. 7419-7430, 2009.

[37] K. Sendur and A. Sahinöz, "Interaction of Radially Polarized Focused Light with a Prolate Spheroidal Nanoparticle," *Opt. Express*, vol. 17, pp. 10910-10925, 2009.

[38] K. Sendur and E. Baran, "Near-Field Optical Power Transmission of Dipole Nano-Antennas," *Appl. Phys. B*, vol. 96, pp. 325-335, 2009.

[39] B. Alavikia and O. M. Ramahi, "Fundamental Limitations on the Use of Open-Region Boundary Conditions and Matched Layers to Solve the Problem of Gratings in Metallic Screens," *Appl. Comput. Electrom.*, vol. 25, pp. 652-658, 2010.

[40] S. S. Abdallah, A. Iolov, K. Bizheva, and O. M. Ramahi, "Effect of Numerical Dispersion in FDTD Simulations of Light Scattering from Photoreceptors," *Appl. Comput. Electrom.*, vol. 25, pp. 388-394, 2010.

[41] K. Sendur and P. Jones, "Effect of Fly Height and Refractive Index on the Transmission Efficiency of Near-Field Optical Transducers," *Appl. Phys. Lett.*, vol. 88, pp. 091110, 2006.

[42] W. E. Moerner and L. Kador, "Optical Detection and Spectroscopy of Single Molecules in a Solid," *Phys. Rev. Lett.*, vol. 62, pp. 2535–2538, 1989.

[43] W. E. Moerner and M. Orrit, "Illuminating Single Molecules in Condensed Matter," *Science*, vol. 283, pp. 1670-1676, 1999.

[44] S. Kühn, U. Hakanson, L. Rogobete, and V. Sandoghdar, "Enhancement of Single-Molecule Fluorescence using a Gold Nanoparticle as an Optical Nanoantenna," *Phys. Rev. Lett.*, vol. 97, pp. 017402, 2006.

[45] S. A. Maier, P. G. Kik, H. A. Atwater, S. Meltzer, E. Harel, B. E. Koel, and A. A. G. Requicha, "Local Detection of Electromagnetic Energy Transport Below the Diffraction Limit in Metal Nanoparticle Plasmon Waveguides," *Nature Mater.*, vol. 2, pp. 229-232, 2003.

[46] S. A. Maier, M. L. Brongersma, P. G. Kik, S. Meltzer, A. A. G. Requiche, and H. A. Atwater, "Plasmonics - Route to Nanoscale Optical Devices," *Adv. Mater.*, vol. 13, pp. 1501-1505, 2001.

[47] S. A. Maier and H. A. Atwater, "Plasmonics: Localization and Guiding of Electromagnetic

Energy in Metal/Dielectric Structures," *J. Appl. Phys.*, vol. 98, pp. 011101, 2005.

[48] T. H. Taminiau, F. D. Stefani, and N. F. van Hulst, "Enhanced Directional Excitation and Emission of Single Emitters by a Nano-Optical Yagi-Uda Antenna," *Opt. Express*, vol. 6, pp. 10858-10866, 2008.

[49] T. Shegai, V. D. Miljkovi, K. Bao, H. Xu, P. Nordlander, P. Johansson, and M. Kall, "Unidirectional Broadband Light Emission from Supported Plasmonic Nanowires," *Nano Lett.*, vol. 11, pp. 706-711, 2011.

[50] A. G. Curto, G. Volpe, T. H. Taminiau, M. P. Kreuzer, R. Quidant, and N. F. van Hulst, "Unidirectional Emission of a Quantum Dot Coupled to a Nanoantenna," *Science*, vol. 329, pp. 930-933, 2010.

Kürşat Şendur received his B.S., M.S., and Ph.D. degrees from Middle East Technical University, Bilkent University, and The Ohio State University, respectively. In 2002, he joined Seagate Technology Research Center, USA where he worked on emerging data storage technologies. Between 2005-2007 he worked at Advanced Microsensors, Boston, USA on thin-film sensor technologies. Since 2007, he has been a faculty member at Sabancı University, Istanbul, Turkey.

Kürşat Şendur received the European Community FP7 Marie Curie International Reintegration Grant in 2007, the Turkish Academy of Sciences Outstanding Young Scientist Award in 2009, the ODTÜ Parlar Foundation Young Researcher Award in 2010, and the İTÜ FABED Foundation Eser Tümen Outstanding Young Scientist Award in 2011.